Streamlining the development of failure surfaces for Fused Filament Fabrication

Gerardo A. Mazzei Capote

A preliminary report submitted in partial fulfillment of
the requirements for the degree of

**Doctor of Philosophy
(Mechanical Engineering)**

at the

University of Wisconsin-Madison

2020

May 2020

Approval

The following thesis, **Defining a failure surface for FFF parts using a novel failure criterion**, developed at the **University of Wisconsin-Madison** has been approved by:

Signature	*Date*

Professor Tim A. Osswald
Department of Mechanical Engineering
College of Engineering
University of Wisconsin-Madison

Abstract

Fused Filament Fabrication (FFF) is arguably the most widely available Additive Manufacturing technology at the moment. Offering the possibility of producing complex geometries in a compressed product development cycle and in a plethora of materials, it comes as no surprise that FFF is attractive to multiple industries, including the automotive and aerospace segments. However, the high anisotropy of parts developed through this technique implies that part failure prediction is extremely difficult —a requirement that must be satisfied to guarantee the safety of the final user. Application of a Failure Criterion to predict part failure can solve this issue. However, a large number of mechanical tests performed under a variety of loading conditions are required to populate the parameters of the function that describes the failure envelope - a process that is extremely time consuming. This research proposal describes a method by which the development of the failure surface can be streamlined, and the number of mechanical tests can be significantly reduced.

Keywords: FFF, FDM, Failure Criteria, Mechanical Testing, Machine Learning.

Table of Contents

Symbols and Acronyms

Acronyms

μCT	Micro Computer Tomography
ABS	Acrylonitrile Butadiene Styrene
AM	Additive Manufacturing
CAD	Computer Aided Design
FC	Failure Criterion
FDM	Fused Deposition Modeling™
FFF	Fused Filament Fabrication
GKC	Gol'denblat-Kopnov Criterion
PA12	Polyamide 12
RP	Rapid Prototyping
SLA	Stereolithography
SLS	Selective Laser Sintering
SSIC	Stress-Stress Interaction Criterion

Symbols

μ^{1112}	SSIC parameter- slope at pure shear failure in the σ_{11} - τ_{12} plane	$-$
μ^{2212}	SSIC parameter- slope at pure shear failure in the σ_{22} - τ_{12} plane	$-$
σ	Axial stress	MPa
σ_{11}	Axial stress in the 1-1 direction	MPa
σ_{22}	Axial stress in the 2-2 direction	MPa

σ_{33}	Axial stress in the 3-3 direction	MPa
τ	Shear stress	MPa
τ_{12}	Shear stress in the 1-2 plane	MPa
τ_{13}	Shear stress in the 1-3 plane	MPa
τ_{23}	Shear stress in the 2-3 plane	MPa
S	Shear strength in the 1-2 plane	MPa
S_{45n}	Negative shear strength for 45° specimen	MPa
S_{45p}	Positive shear strength for 45° specimen	MPa
X_c	Compressive strength in the 1-1 direction	MPa
X_t	Tensile strength in the 1-1 direction	MPa
Y_c	Compressive strength in the 2-2 direction	MPa
Y_t	Tensile strength in the 2-2 direction	MPa

List of Figures

List of Tables

Introduction

Additive Manufacturing (AM) is an umbrella term that encompasses all fabrication techniques where the final geometry of the part is obtained through superposition of material in a layer-by-layer basis [1]. Developed in the 1980s, this manufacturing technique permits immensely shorter part development cycles, since the transition from a 3D *Computer Aided Design* (CAD) to part fabrication only requires one intermediate step: the use of a slicing engine that converts the geometry of the object into machine instructions [1]. For this reason, AM technologies were initially employed exclusively for prototype development and were referred to as *Rapid Prototyping techniques* (RP). However, recent innovations in the field have caused AM to be considered as a legitimate manufacturing technology since it is also capable of reproducing complex geometries unattainable through traditional methods [1].

While offering great advantages over traditional part fabrication methods, AM comes with its own set of limitations and disadvantages: First and foremost, the use of a stratified build approach tends to produce extremely anisotropic parts. Secondly, the geometric accuracy of the object produced is highly dependent of process parameters, particularly, the thickness of the layers. Finally, as of the time of this writing, AM lacks the standardization and scrutiny that are associated to most traditional manufacturing techniques [1].

Fused Filament Fabrication (FFF), also known under the trademark *Fused Deposition Modeling* (FDM™), represents perhaps the most prevalent AM technique in the market due to the advent of low-cost, desktop 3D printers in the early 2010s [2]. Due to the broad availability of machines and relatively low costs of material, there is a surging interest in optimizing FFF to produce small batches of end-user grade parts. Success stories are varied, but examples include vacuum form molds, fixtures, jigs, and tools used to aid assembly lines in the automotive industry [3, 4, 5]. However, this technology still faces the challenges and limitations that currently affect the field of AM as a whole. Namely, anisotropy introduced through the layer-by-layer build approach makes it difficult to assess the expected mechanical behavior of FFF parts when subjected to important mechanical stresses [2]. For these reasons, multiple attempts have been made to characterize the anisotropy of FFF manufactured objects, such as the studies performed by Koch *et al.* [6] and Rankouhi *et al.* [7], which show that the ultimate tensile strength of FFF coupons is sensitive to process parameters such as the layer thickness and, in particular, the orientation in which the plastic strands are laid during the build process -henceforth referred to as the bead orientation. Literature related to preventing failure through the use of *Failure Criteria* (FC) in the design stages is scarce, given the difficulty of using commercially available FFF machines to produce test coupons with unconventional bead orientations, as well as the limitations inherent to development of failure envelopes. The large number of coupons required to properly characterize the failure behavior of parts is one of the main culprits for the small number of research articles on the topic. However, recent efforts include the developments of failure envelopes for *Polyamide 12* (PA12) used in *Selective Laser Sintering* (SLS) [8], and more importantly for this body of work, a failure surface for *Acrylonitrile Butadiene Styrene* (ABS) used in FFF [9]. For the latter, certain test specimens in unconventional configurations had to be produced using a unique off-axis 3D printer developed in-house. In both cases, the researchers utilized a FC that incorporates stress interactions into the calculations of the failure surface, a feature that more recognized criteria, such as the Tsai-Wu model fail to take into account [10].

This research proposal springboards from the failure surface developed for FFF using ABS developed by Mazzei Capote *et al.* [9].

This work offers a comprehensive overview of AM technologies, FFF and shortcomings of current failure criteria in Chapter 1. Chapter 2 details the failure criterion used throughout this work, as well as outlining its advantages over similar models. Chapters **??** through **??** detail the experimental setup followed, as well as outlining noteworthy results. Finally, conclusions and recommendations are given in Chapter **??** in the hopes of guiding future work on the topic.

1 Background

1.1 Additive Manufacturing

Additive Manufacturing (AM) technologies had their beginnings in the decade of the 1980s. During this time, various independently developed patents were filed across the globe, describing a process that would construct an object by selectively adding layers of material -as opposed to removing excess matter or deforming mass to obtain a desired shape. This represents the core definition of AM: any technology where the final geometry of the manufactured object is obtained through controlled addition of material qualifies as an Additive Manufacturing technique [1].

Advancements in the fields of computing, *Computer Aided Design* (CAD), and controllers, among other technological developments, were necessary to translate the patents into working prototypes, with some eventually becoming the foundations of commercially successful companies -such as 3D Systems in 1986 and Stratasys in 1989 [1, 11, 12]. The basic process of AM has remained largely unchanged from its first iteration in the late 80s: First, a computer model of the object is made using CAD software and exported under the *.stl* file format. Afterwards, the part geometry is stratified, or "sliced", and translated into machine instructions using a specialized software called *slicing engine*. An AM machine then follows said instructions, commonly referred to as the *toolpath*, to build the object in layers. Finally, the part is available to the user. Depending on either the requirements of the part, or the specifics of the AM technique used, some post-processing may be required [1]. A visual representation of the process is shown in Figure 1.1.

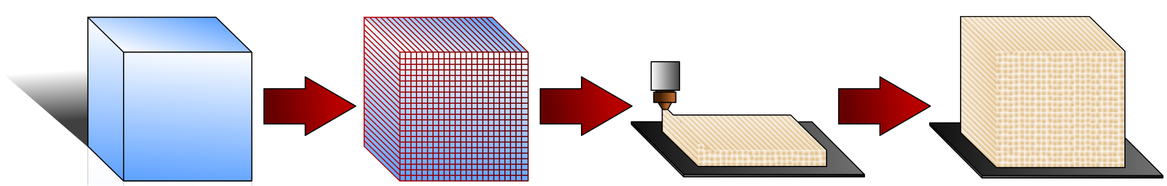

(a) CAD model (b) Slicing (c) Building Process (d) Finished part

Figure 1.1: Process flow of AM

While all AM technologies operate on the same basic process flow described above, the specifics of each AM technique vary substantially, ranging from processes that use paper and binder, all the way through metal-based, laser tracing technologies. Since this is a rapidly evolving field, no general consensus exists for classifying the multiple AM processes available as of the time of this writing. However, the classification system proposed under the ASTM/ISO 52900 standard [13], has been somewhat accepted by the field and divides AM technologies as follows:

1. **Binder Jetting**: AM techniques where a binding agent is used to selectively promote cohesion in powder materials -generally gypsum, sand or metallic powders [13, 14].

2. **Directed Energy Deposition**: AM processes where a focused thermal energy source (i.e. laser, electron beam, plasma arc) is used to fuse materials as they are being deposited in the build volume. Materials are almost exclusively metals [13, 14].

3. **Material Extrusion**: In this type of AM technology, material is dispensed through a nozzle or orifice. Fused Filament Fabrication belongs to this classification. Materials are almost exclusively thermoplastics [13, 14].

4. **Material Jetting**: AM techniques where build material is deposited selectively in droplets. Materials are usually wax or thermoplastics, but there are examples of metal-based, material jetting techniques [13, 14].

5. **Powder Bed Fusion**: AM processes where portions of a powder bed are selectively fused through application of thermal energy. *Selective Laser Sintering* (SLS) belongs to this category. Materials are usually thermoplastic polymers or metals [13, 14].

6. **Sheet Lamination**: In this type of AM technology, the final part is formed by bonding sheets of material -usually paper or composites [13, 14].

7. **Vat Photopolymerization**: In this AM process, a liquid photopolymer is selectively cured by a light source. *Stereolithography* (SLA), arguably the first AM technology, belongs to this category. Due to the nature of this technique, the only materials used are photopolymers [13, 14].

1.1.1 Advantages and Disadvantages of AM

Since AM processes allow a relatively direct conversion of a CAD model into a constructed object, they were originally exclusively used for prototype development. For this reason, they were initially classified as "*Rapid Prototyping*" (RP) technologies. This terminology is still used today, however, it is being superseded by *Additive Manufacturing* since its potential to become a proper fabrication technique exists [1]. While being capable of quickly jumping from part design to manufacturing is a great advantage, AM has its own set of drawbacks. Table 1.1 summarizes the most noteworthy set of advantages and disadvantages typical of most AM technologies.

Table 1.1: Advantages and Disadvantages of Additive Manufacturing

Advantages	**Disadvantages**
Faster product development cycles [1]	Part quality highly dependent on process parameters [1]
No additional tools needed for part fabrication[1]	Stratified build generally results in anisotropic parts [1, 2]
Cost effective for small batches of parts [15, 16, 17]	Costly for production of more than hundreds of parts [15, 16, 17]

Out of all the described advantages and disadvantages, the high anisotropy of AM parts is responsible for the slow embrace of AM in highly demanding engineering fields -such as the aerospace and automotive industries. The highly anisotropic mechanical behavior makes it extremely difficult to predict part failure, therefore, it cannot be implemented in engineering applications where catastrophic failure is to be avoided at all costs. Even so, success stories of implementation of AM in industrial environments are abundant. Relatively recent examples include the use of FFF machines to manufacture tools, jigs, and fixtures in a Volkswagen assembly plant in Europe [5]; production of a complex fuel nozzle injector for the LEAP jet engine, using powder based, metal AM by GE [18]; and development and production of highly optimized, 3D printed midsoles for high performance running sneakers by companies as large as New Balance and Adidas [19, 20, 21]. Note that in the cases presented, the main reason behind the usage of AM was either reduction of expenses associated with producing small batches of parts, or the capability of reproducing a unique and complex geometry. This is a trend that is observed in most of the literature describing implementation of AM into industrial scenarios.

While the advantages and disadvantages described here cover the field of AM as a whole, each technique comes with its own set of pros and cons that may make it the preferred method to reproduce a particular product or geometry. This work, however, focuses solely on FFF. The specifics of this process are described in detail in Section 1.2.

1.2 Fused Filament Fabrication

Fused Filament Fabrication (FFF) is an AM technology where the final geometry of the part is obtained through controlled extrusion of a liquid, self-hardening material -usually a thermoplastic polymer in molten state [1]. Originally developed by Stratasys in the 1980s under the still trademarked *Fused Deposition Modeling* (FDM™) moniker, it has recently become one of the most widely used AM techniques due to the advent of low-cost, desktop FFF machines in the early 2010s caused by the expiration of key patents from Stratasys [1, 2].

1.2.1 The FFF process

At its core, the typical FFF machine consists of a heated build surface commonly referred to as a *build plate*, a specialized tool known as a *printhead*, and the fabrication material -supplied in the form of spools of thermoplastic polymer filament. The printhead is itself composed of a heating element, a nozzle, and some form of driving mechanism that pushes the filament downward. As the thermoplastic material is moved through the heated chamber, polymer melt is formed and extruded through the opening at the tip of the nozzle, producing a *bead*. The molten polymer can then be deposited upon the build plate, where controlled movements of the printhead and the fabrication surface gradually construct the final geometry of the part in a layer-by-layer build approach [1]. The typical setup of an FFF machine can be seen in Figure 1.2. In this example, the printhead moves in the x-y plane, while the build plate moves in the z direction.

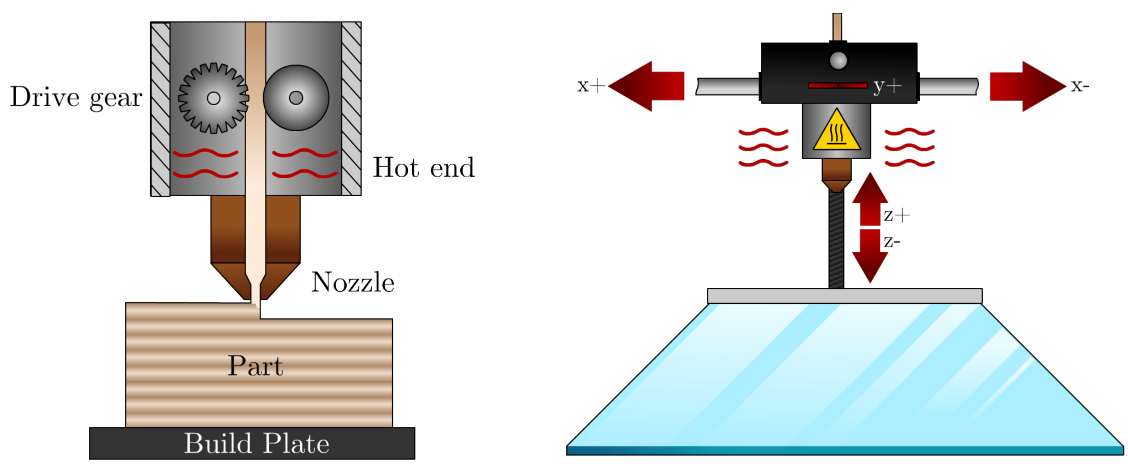

(a) FFF printhead cross section

(b) Typical FFF machine

Figure 1.2: The basic FFF machine configuration

Like all AM technologies, the FFF process starts in a computer with a CAD model converted to the *.stl* file format. The geometry is then translated to machine instructions through a *slicing engine*, where the user inputs a plethora of process parameters that include nozzle and build plate temperatures, print speed, layer thickness, and build orientation. Finally the *toolpath* is executed by the FFF printer, building the object in a layer-by-layer basis – sometimes referred to as *2.5D* printing [1, 4]. Figure 1.3 shows an abridged version of the process. The z axis indicates the intended build direction. Note how some of the finer details in the original CAD file are lost in the printed part – due in part to the layer height and build orientation selected.

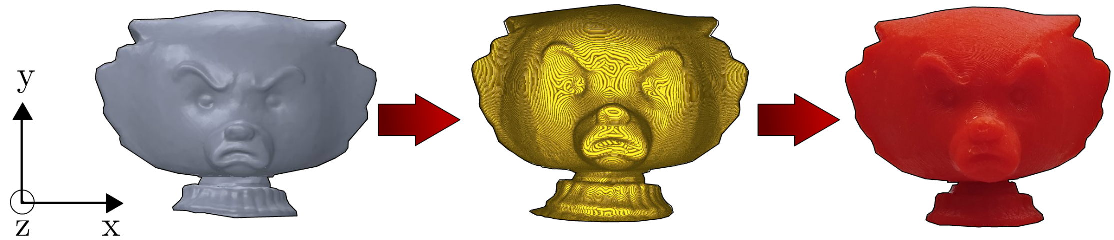

Figure 1.3: Model, toolpath and final part in the FFF process

The process is capable of producing complex geometries that would be otherwise hard to reproduce through other polymer processing techniques, such as injection molding. However, it is bound by the disadvantages described in Section 1.1.1, as well its own unique set of drawbacks. Namely:

- The circular orifice in the nozzle makes FFF incapable of reproducing sharp corners, limits the size of the smallest reproducible feature, and causes the final part to be filled with voids –originating in the junction of round beads. These problems can be seen in Figure 1.4: On the left, a comparison of a 90° corner planned in the toolpath and the final geometry of the printed bead is shown. Note the rounded nature of the turn. On the right, a cross section of an FFF part obtained through *Micro Computer Tomography* (μCT) shows the voids that form during the printing process.

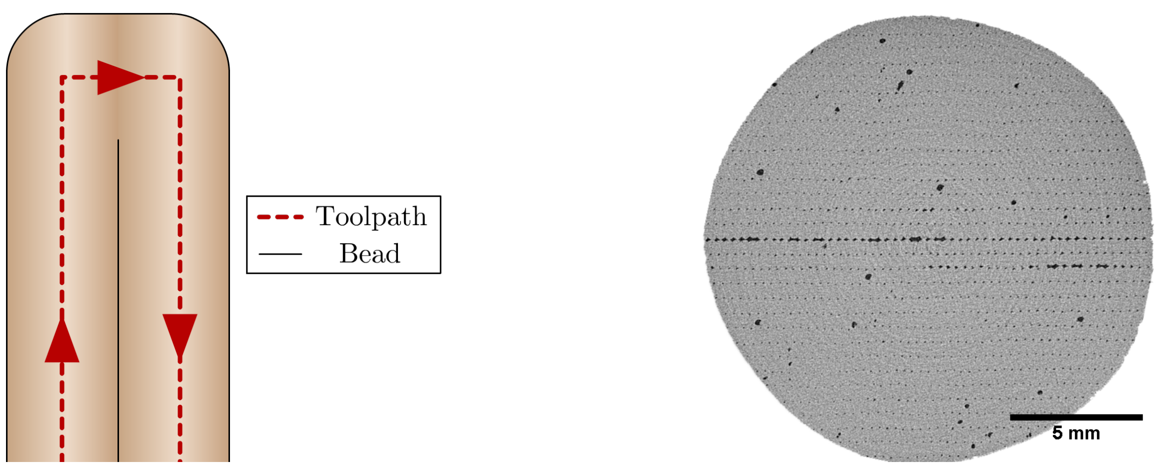

(a) FFF toolpath vs. printed bead

(b) Cross section of an FFF part

Figure 1.4: Typical FFF part mesostructure and its origin

- The junction of adjacent beads behaves akin to a polymeric weld, and has inferior mechanical properties than the bulk material [2]. This, coupled with the aforementioned voids which can act as stress concentrators, causes FFF parts to behave in extremely anisotropic manner with diminished mechanical performance when compared to analogous parts obtained through traditional polymer processing technologies – such as injection molding [2].

This last disadvantage is responsible for the slow embrace of FFF as a proper manufacturing technique: the high anisotropy of FFF parts imply that predicting part failure becomes extremely difficult and thus, proper part design that guarantees safe operation of the object under important loads is hard to achieve. For this reason, efforts to characterize the mechanical behavior of FFF parts have existed since as early as the 1990s. Recent examples are presented in Section 1.2.2.

1.2.2 Mechanical Properties of FFF parts

Efforts have been made to characterize the mechanical anisotropy of FFF parts. However, due to the lack of testing standards and problems during toolpath planning, most studies focus solely in the tensile mechanical performance of FFF coupons.

Studies performed by Koch *et al.* [6] and Rankouhi *et al.* [7] indicate that the final tensile properties of FFF coupons are particularly sensitive to bead orientation and proper mass output through the nozzle. Other process parameters, such as the layer thickness, have varying degrees of impact upon the final tensile strength of the part. In both studies, tensile coupons were printed with bead orientations of 0°, 45° and 90° in the x-y plane. Results showed that in all the experimental conditions selected, a 0° orientation always behaved closer to the bulk material, whereas a 90° sample always had significantly lower tensile strengths. The 45° samples sat between both extremes. It is important to note that in both studies, toolpath manipulation was necessary to avoid premature failure of the coupons due to stress concentrators originating in void formation due to the elliptical nature of the beads. Figure 1.5 shows some of the results by Koch *et al.* The geometry corresponds to an ASTM Type I Tensile coupon. Injection molded results are denoted *IM* for comparison. Note that the 90° orientation had a tensile strength that was 25% inferior to the IM counterpart, and 20% worse than the 0° oriented FFF coupon. This is a prevalent trend in the consulted bibliography.

Literature for other types of mechanical testing of FFF parts is relatively scarce when compared to tension experiments. Research indicates that the compressive strength of FFF parts tends to be higher than the tensile strength, as well as being less sensitive to process parameters —the bead orientation in particular seems to have a significantly diminished impact upon the compressive strength when compared to its effect upon tensile tests [22, 23]. Shear strength results are virtually non-existent.

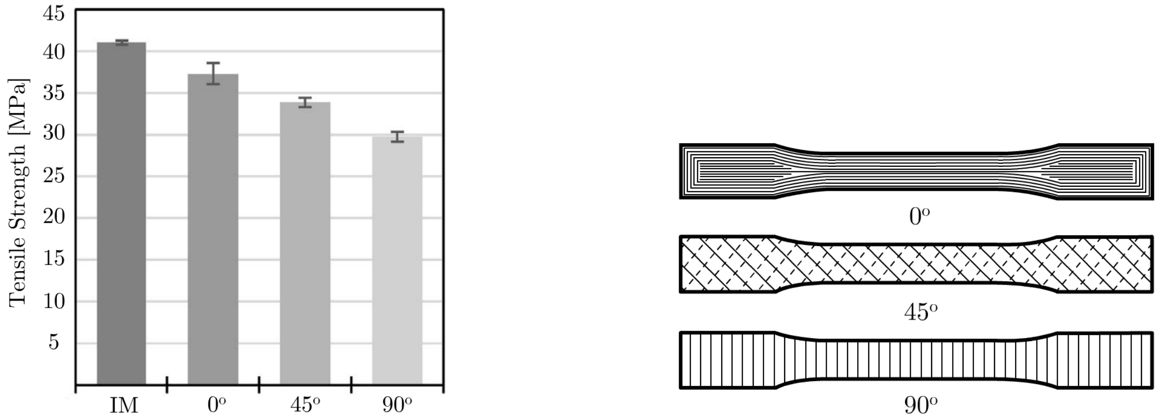

(a) Tensile strength of tensile coupons

(b) Representation of coupons used

Figure 1.5: Results from Koch *et al.* [6]

1.3 Failure Criteria

The increased use of advanced materials in industry has brought upon a necessity to properly characterize their strengths and failure modes. Composites in particular are commonly used in highly demanding engineering fields given that they excel in mechanical properties. However, due to their nature, their behavior is extremely anisotropic. For this reason, it has been of great interest to develop a proper way to model the behavior of anisotropic materials under mechanical stresses as a way to predict part failure – a practice from here on referred to as developing a *failure criterion*.

Early attempts to properly predict failure of anisotropic materials go as far back as 1948 with the Hill model [10]. Further developments led to a plethora of failure criteria, such as the Tsai-Hill, Malmeister, Tsai-Wu, Gol'denblat-Kopnov, Puck, and Cuntze to name a few [10, 24]. A wide variety of criteria exists because a model will rarely capture the complete failure behavior of an anisotropic material. To illustrate this point, refer to Figure 1.6, reproduced from work by Sun *et al.* [25] where a composite glass fiber and epoxy laminate was loaded biaxially, in a direction that was either parallel (σ_{11}), perpendicular (σ_{22}) to the fiber, or a combination of both. Positive stresses indicate tensile load, while negative values point to compressive forces. The data, represented by the white squares, does not agree with any of the used models in the fourth quadrant of the graph. This type of behavior is common throughout the literature: Puck's model is great at predicting shear strengthening effects, but doesn't perform well when dealing with combined axial loading scenarios; the Gol'denblat-Kopnov model by contrast is great at predicting axial stress interactions, but falls short when dealing with shear strengthening effects caused by combined shear-axial loadings. These trends point to the limitations of each model: in order to either facilitate calculations, or due to the difficulty of performing combined loading tests, interaction effects are neglected either by mathematical choice, or indirectly through the inner workings of the failure criterion [10].

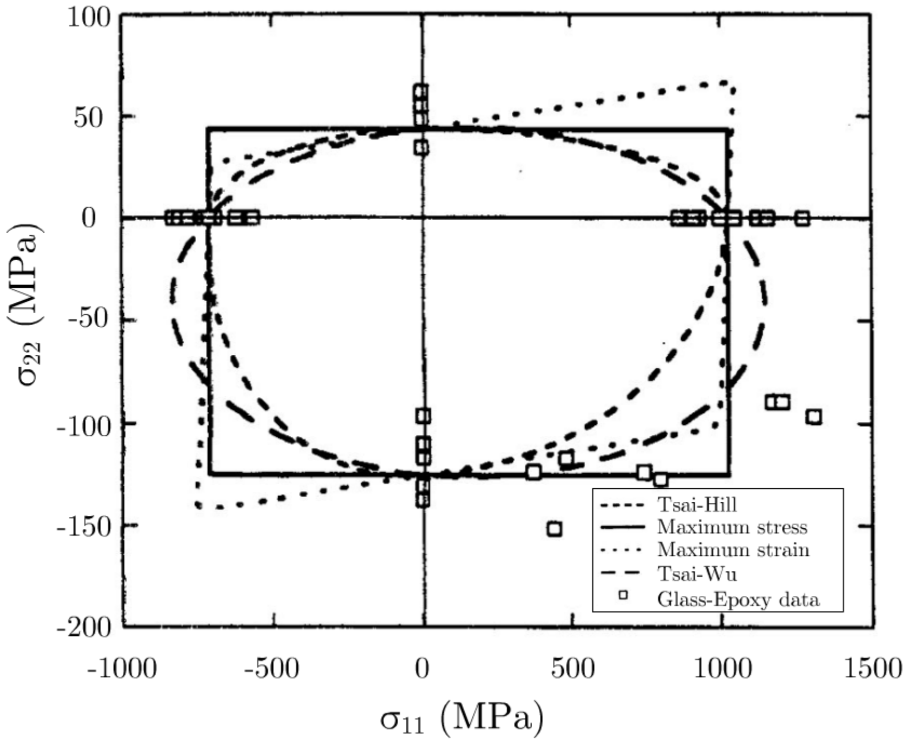

Figure 1.6: Comparison of different failure criteria. [25]

Properly mapping a failure surface through a criterion proves to be an invaluable tool for design, since it allows engineers to assess if a part will perform safely under its intended loading conditions. Such tool could in theory help overcome the main shortcoming of FFF since a properly tailored failure envelope would allow proper part design considerations. Chapter 2 describes in detail an approach based on the Gol'denblat-Kopnov model that includes interaction effects to properly describe the failure behavior of anisotropic parts. This chapter will also go into detail describing how this FC was applied to develop a failure envelope for FFF.

2 Use of Failure Criteria for AM

As described during Section 1.3 of Chapter 1, currently available failure criteria fail to completely integrate interaction effects into the modeled failure behavior of anisotropic materials. In 2017, Paul and Tim Osswald proposed a model that attempts to overcome these limitiations [10]. This recent failure criterion has the following characteristics:

- **Tensor based and purely mathematical**: as opposed to phenomenological or mechanistic models such as the Puck or Cuntze failure criteria.
- **Based on the Gol'denblat-Kopnov model**.
- **Includes stress interactions that other models neglect**.

Originally titled "A Strength Tensor Based Failure Criterion with Stress Interactions", it will be referred in this work as the Stress-Stress Interaction Criterion (SSIC). This chapter will briefly describe the Gol'denblat-Kopnov model upon which the SSIC is based, followed by a proper description of how it implements stress interactions. Finally, it will go detail how it was used to develop a failure envelope for FFF parts produced with ABS.

2.1 The Gol'denblat-Kopnov Model

The Gol'denblat-Kopnov Criterion (GKC) describes a mathematical function that depends on the stress state of an anisotropic material. Should the computation of this expression exceed a threshold, part failure is to be expected. To that end, a scalar function that depends on stress tensors that completely characterize the state of the material was developed [26]. This function is shown in Equation 2.1, where stresses are denoted σ, and the subindices i,j,k,l denote a particular load direction.

$$f = (F_{ij}\sigma_{ij})^{\alpha} + (F_{ijkl}\sigma_{ij}\sigma_{kl})^{\beta} + (F_{ijklmn}\sigma_{ij}\sigma_{kl}\sigma_{mn})^{\gamma} + ... \tag{2.1}$$

The terms F_{ij}, F_{ijkl} and F_{ijklmn} represent second, fourth and sixth order tensors respectively. These terms of the equation depend on engineering strength parameters, such as the ultimate tensile and compressive strengths of the material in a particular load direction [10]. Due to the complexity associated with using higher order tensors, Gol'denblat and Kopnov limited their approach to using only the second and fourth order terms. Thus Equation 2.1 is reduced to:

$$f = (F_{ij}\sigma_{ij})^{\alpha} + (F_{ijkl}\sigma_{ij}\sigma_{kl})^{\beta} \tag{2.2}$$

In order to attain a linear criterion scalar function, the exponents α and β were assigned values of 1 and 1/2 respectively. Finally, in plane stress scenarios, the GKC becomes:

$$\begin{aligned} f = F_{11}\sigma_{11} + F_{22}\sigma_{22} + F_{12}\tau_{12} + (F_{1111}\sigma_{11}^2 + F_{2222}\sigma_{22}^2 + F_{1212}\tau_{12}^2 \\ +2F_{1122}\sigma_{11}\sigma_{22} + 2F_{1112}\sigma_{11}\tau_{12} + 2F_{2212}\sigma_{22}\tau_{12})^{1/2} \end{aligned} \tag{2.3}$$

Note that in Equation 2.3 σ and τ denote normal and shear stresses respectively. Figure 2.1 depicts an anisotropic material and all the possible loading directions for reference.

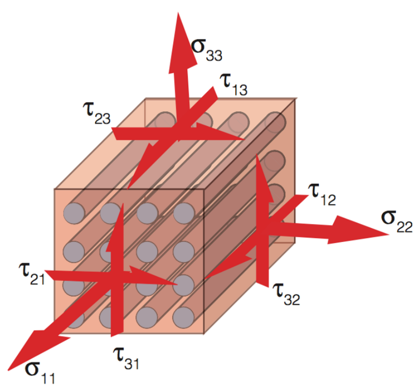

Figure 2.1: Different load directions in an anisotropic material

Per Gol'denblat and Kopnov's design, should the computation of f in Equation 2.3 be greater or equal to 1, part failure is to be expected. However, to simplify calculations, they deliberately assumed the interaction terms F_{1112} and F_{2212} to be zero. This is an important consideration that will come into play when describing the SSIC.

Most of the terms in the GKC are obtained through mechanical testing of coupons under pure uniaxial loads in the 1 or 2 direction, or pure shear in the 1-2 plane [10]. In these scenarios, f will be equal to 1 at failure, and the stress state will be known to the user, allowing some of the unknown tensorial parameters to be easily calculated. Using F_{11} and F_{1111} as examples, the process would be as follows:

1. The tensile and compressive strength in the 1-1 direction would be obtained through mechanical testing. These values are named X_t and X_c respectively.

2. Under these failure conditions, Equation 2.3 is reduced to the following system of equations:
$$\begin{cases} 1 = \quad F_{11}X_t + (F_{1111}X_t^2)^{1/2} \\ 1 = -F_{11}X_c + (F_{1111}X_c^2)^{1/2} \end{cases}$$

3. F_{11} and F_{1111} can be obtained, yielding $F_{11} = \frac{1}{2}(\frac{1}{X_t} - \frac{1}{X_c})$ and $F_{1111} = \frac{1}{4}(\frac{1}{X_t} + \frac{1}{X_c})^2$.

The only exception to this procedure would be the F_{1122} component, which requires measuring the positive and negative shear strengths of a coupon with reinforcement oriented in 45°. These parameters are named S_{45p} and S_{45n} respectively. Table 2.1 summarizes the nomenclature used for the strength parameters required to completely populate the failure function of the GKC. Table 2.2 summarizes all the tensorial component calculations.

Table 2.1: Nomenclature of the GKC parameters

Parameter	**Description**
X_t	Tensile strength in the 1-1 direction
X_c	Compressive strength in the 1-1 direction
Y_t	Tensile strength in the 2-2 direction
Y_c	Compressive strength in the 2-2 direction
S_{45p}	Positive shear strength for 45° specimen
S_{45n}	Negative shear strength for 45° specimen
S	Shear strength in the 1-2 plane

Table 2.2: Tensorial components of the GKC

Component	**Formula**
F_{11}	$\frac{1}{2}(\frac{1}{X_t} - \frac{1}{X_c})$
F_{1111}	$\frac{1}{4}(\frac{1}{X_t} + \frac{1}{X_c})^2$
F_{22}	$\frac{1}{2}(\frac{1}{Y_t} - \frac{1}{Y_c})$
F_{2222}	$\frac{1}{4}(\frac{1}{Y_t} + \frac{1}{Y_c})^2$
F_{12}	0
F_{1212}	$\frac{1}{S^2}$
F_{1122}	$\frac{1}{8}[(\frac{1}{X_t} + \frac{1}{X_c})^2 + (\frac{1}{Y_t} + \frac{1}{Y_c})^2 - (\frac{1}{S_{45p}} + \frac{1}{S_{45n}})^2]$

2.2 The Stress-Stress Interaction Criterion

One of the assumptions made in the GKC is that the components F_{1112} and F_{2212} in Equation 2.3 are null. While this simplifies the model, it essentially neglects any interactions between axial loads and shear stresses, namely, the σ_{11} - τ_{12} and σ_{22} - τ_{12} interactions. Practically, this causes the failure surface developed through the GKC to under-predict shear strengthening effects exhibited by anisotropic materials loaded in combined axial and shear conditions. Figure 2.2 shows a comparison between experimental data obtained from the first World Wide Failure Exercise (WWFE-I) and the GKC envelope developed for this material. In this example, a unidirectional glass reinforced epoxy composite was tested in multiple loading conditions in the σ_{22} and τ_{12} stress plane. White circles indicate average values for pure uniaxial or shear scenarios. Note how on the first quadrant, the model follows the data closely. However, in the second quadrant, the criterion is relatively conservative, failing to capture the strengthening that occurs when loading the material in compression and shear.

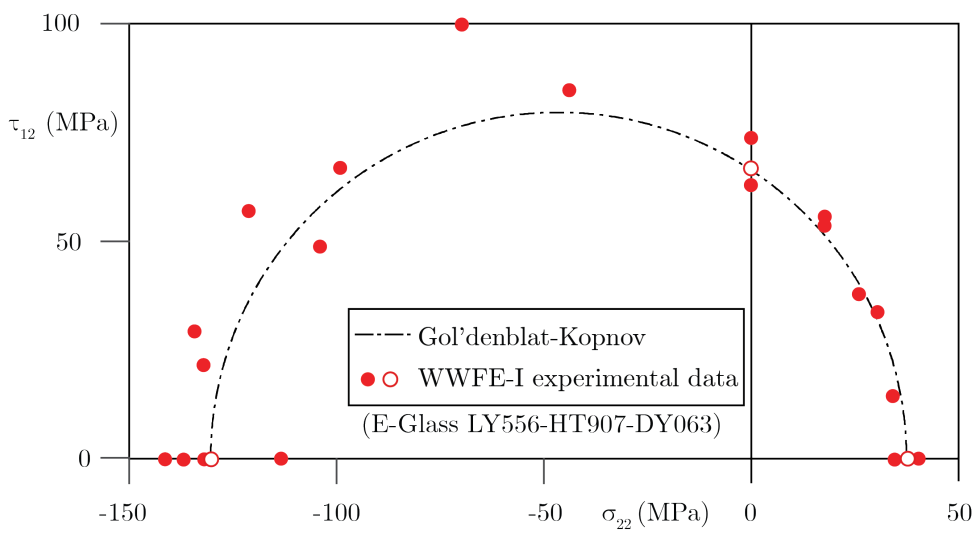

Figure 2.2: GKC failure surface developed using data from the WWFE-1 [10]

The Stress-Stress Interaction Criterion (SSIC) attempts to overcome these limitations by building upon the GKC. For the SSIC, the interaction effects are captured through the use of the slopes of the failure surface at any of the points where the engineering strength is known within a particular stress plane [10]. In this failure scenario, the stress state of the coupon is known and easy to implement into Equation 2.3, where $f = 1$. The resulting expression can then be derived with respect to one of the stresses, allowing for the interaction components to be calculated. This is better illustrated through an example. Assuming the component of interest is F_{2212}, the procedure to calculate it through the SSIC would be as follows:

1. Obtain all the tensorial components possible through the GKC.

2. Using the σ_{22}–τ_{12} stress plane, take the derivative of Equation 2.3 as a function of σ_{22} in the scenario of failure under pure shear ($f = 1$). This yields the expression:

$$0 = F_{22} + [F_{1212}S(\frac{d\tau_{12}}{d\sigma_{22}}) + F_{2212}S] \tag{2.4}$$

   where $\frac{d\tau_{12}}{d\sigma_{22}}$ is the slope of the graph at failure under shear. This term is named μ^{2212} in the SSIC and can be obtained by performing combined loading tests. Refer to Figure 2.3 for a visual representation.

3. Rearranging Equation 2.4 to solve for the unknown F_{2212} gives the following expression:

$$F_{2212} = -\frac{F_{22}}{S} - F_{1212}\mu^{2212} \tag{2.5}$$

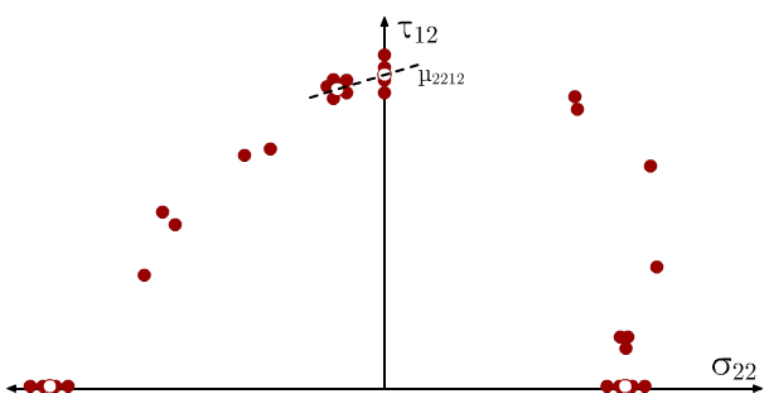

Figure 2.3: μ^{2212} parameter in the τ_{12} - σ_{22} plane

A similar procedure can be followed for any σ_{ii}-τ_{ij} interaction, or even any σ_{ii}-σ_{jj} components. For this last scenario, the user has four potential choices of slopes to determine the tensorial component of interest. In the OOC, any slope obtained from a σ_{ii}-σ_{jj} stress plane is named λ^{iijj}, as opposed to μ^{iiij} for slopes in a σ_{ii}-τ_{ij} reference. A schematic of all possible λ^{iijj} is shown in Figure 2.4, while Table 2.3 summarizes all the possible interaction factors available through the SSIC, where τ_{ij}^{u} denotes ultimate shear strength in a particular shear plane.

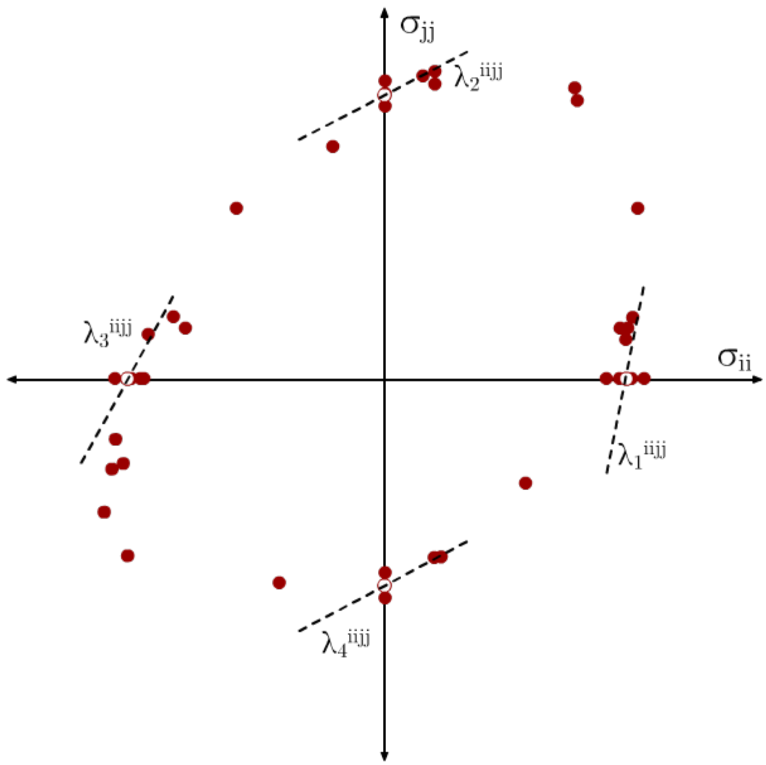

Figure 2.4: λ^{iijj} parameters in a generic σ_{ii} - σ_{jj} stress plane

Table 2.3: Interaction components attainable through the SSIC [10]

Component	**Formula**
F_{iiij}	$-\frac{F_{ii}}{\tau^u_{ij}} - F_{ijij}\mu^{iiij}$
F_{iijj} through λ_1^{iijj}	$-\frac{(F_{ii}+F_{jj}\lambda_1^{iijj})F_{iiii}^{1/2}+F_{iiii}}{\lambda_1^{iijj}}$
F_{iijj} through λ_2^{iijj}	$-(F_{ii}+F_{jj}\lambda_2^{iijj})F_{jjjj}^{1/2} - F_{jjjj}\lambda_2^{iijj}$
F_{iijj} through λ_3^{iijj}	$\frac{(F_{ii}+F_{jj}\lambda_3^{iijj})F_{iiii}^{1/2}-F_{iiii}}{\lambda_3^{iijj}}$
F_{iijj} through λ_4^{iijj}	$(F_{ii}+F_{jj}\lambda_4^{iijj})F_{jjjj}^{1/2} - F_{jjjj}\lambda_4^{iijj}$

Applying the SSIC to the data shown in Figure 2.2 demonstrates how the failure surface developed through this new criterion better reflects the failure behavior than its GKC counterpart. A comparison between the two can be seen in Figure 2.5. Note how the SSIC envelope captures the shear strengthening better than the GKC.

The SSIC offers a way of capturing in a more accurate manner the different failure modes of parts produced through AM technologies. As an example, the model has been successfully implemented by Obst *et al.* in 2018 for SLS manufactured parts produced

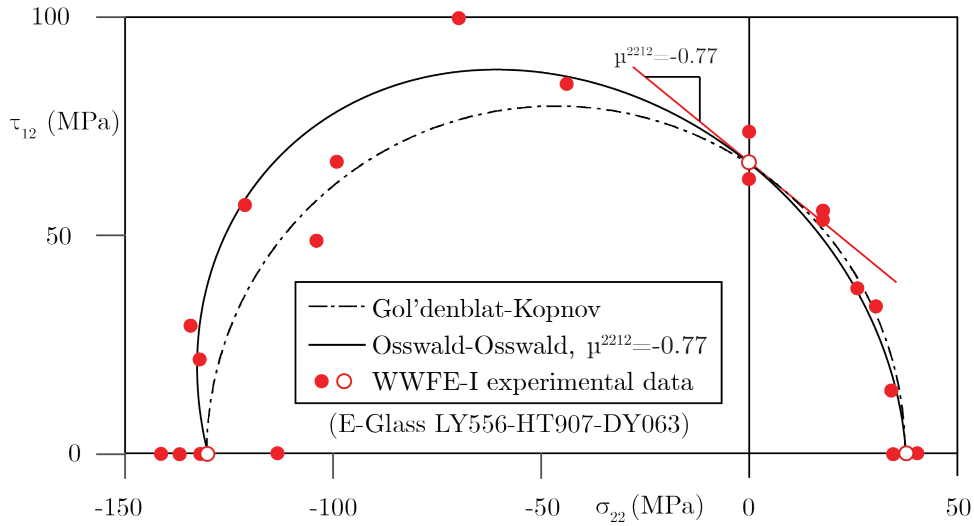

Figure 2.5: Comparison of GKC and SSIC failure envelopes [10]

with PA12 [8, 27]. Their results show how the model was able to capture the τ_{12}-σ_{22} and σ_{11}-σ_{22} interactions. The failure surface obtained is shown in Figure 2.6.

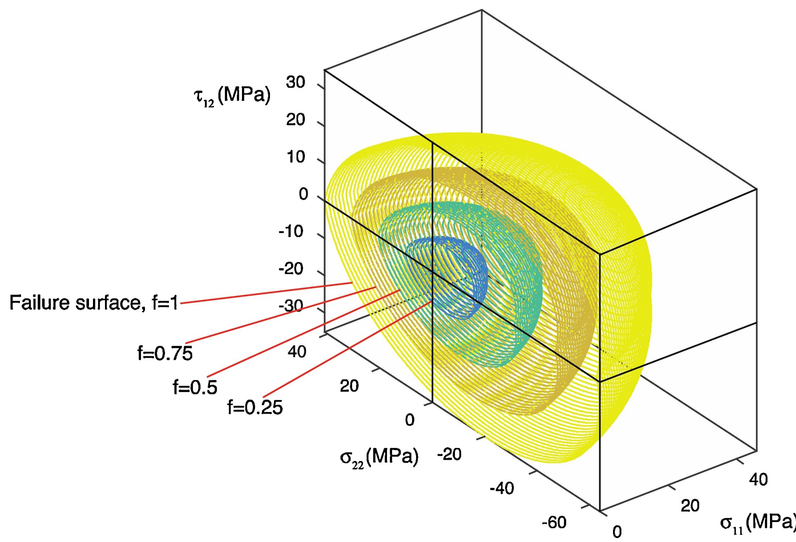

Figure 2.6: Failure surface for SLS developed through the SSIC [8]

This work will apply the SSICC to FFF, in the hopes that it becomes a tool for safely designing parts intended to be manufactured through this process. Chapter ?? will detail the material and experimental methods used to achieve this goal.

Bibliography

[1] Ian Gibson, David Rosen, and Brent Stucker. *Additive Manufacturing Technologies*. 2nd Ed. Springer, 2015. ISBN: 978-1-4939-2112-6. DOI: 10.1007/978-1-4939-2113-3. URL: http://link.springer.com/10.1007/978-1-4939-2113-3.

[2] G A Mazzei Capote, A Redmann, C Koch, and N Rudolph. "Towards a Robust Production of FFF End-User Parts with Improved Tensile Properties". In: *Proceedings of the 28th Annual International Solid Freeform Fabrication Symposium*. Austin, TX, 2017, pp. 507–518.

[3] Cole Hartman and Veronica de la Rosa. *Benefits of 3D Printing Vacuum Form Molds*. 2014. URL: http://studiofathom.com/wp-content/uploads/Vacuum-Forming-White-Paper-F001-5-1-2014.pdf (visited on 02/06/2018).

[4] Luke Van Hulle. "Robotic Off-Axis Fused Filament Fabrication". Master Thesis. University of Wisconsin-Madison, 2017.

[5] Caspar de Vries. *Volkswagen Autoeuropa: Maximizing production efficiency with 3D printed tools, jigs, and fixtures*. 2017. URL: https://ultimaker.com/en/stories/43969-volkswagen-autoeuropa-maximizing-production-efficiency-with-3d-printed-tools-jigs-and-fixtures (visited on 02/02/2018).

[6] Carsten Koch, Luke Van Hulle, and Natalie Rudolph. "Investigation of mechanical anisotropy of the fused filament fabrication process via customized tool path generation". In: *Additive Manufacturing* 16 (2017), pp. 138–145. ISSN: 22148604. DOI: 10.1016/j.addma.2017.06.003. URL: http://dx.doi.org/10.1016/j.addma.2017.06.003.

[7] Behzad Rankouhi, Sina Javadpour, Fereidoon Delfanian, and Todd Letcher. "Failure Analysis and Mechanical Characterization of 3D Printed ABS With Respect to Layer Thickness and Orientation". In: *Journal of Failure Analysis and Prevention* 16.3 (2016), pp. 467–481. ISSN: 15477029. DOI: 10.1007/s11668-016-0113-2.

[8] P. Obst, M. Launhardt, D. Drummer, P.V. Osswald, and T.A. Osswald. "Failure criterion for PA12 SLS additive manufactured parts". In: *Additive Manufacturing* 21.March (2018), pp. 619–627. ISSN: 22148604. DOI: 10.1016/j.addma.2018.04.008. URL: http://linkinghub.elsevier.com/retrieve/pii/S221486041830099X.

[9] Gerardo A Mazzei Capote, Natalie M Rudolph, Paul V Osswald, and Tim A Osswald. "Failure surface development for ABS fused filament fabrication parts". In: *Additive Manufacturing* 28.April (2019), pp. 169–175. ISSN: 2214-8604. DOI: 10.1016/j.addma.2019.05.005. URL: https://doi.org/10.1016/j.addma.2019.05.005.

[10] Paul V. Osswald and Tim A. Osswald. "A strength tensor based failure criterion with stress interactions". In: *Polymer Composites* (2017). ISSN: 15480569. DOI: 10.1002/pc.24275. arXiv: 1206.4529. URL: http://onlinelibrary.wiley.com/doi/10.1002/pc.24275/fullhttp://doi.wiley.com/10.1002/pc.24275.

[11] 3D Systems. *Our Story*. 2017. URL: https://www.3dsystems.com/our-story (visited on 02/15/2018).

[12] Stratasys. *About us*. 2017. URL: http://www.stratasys.com/corporate/about-us (visited on 02/15/2018).

[13] ASTM International and International Organization for Standardization. *ISO/ASTM 52900:2015-Standard Terminology for Additive Manufacturing- General Principles-Terminology*. West Conshohocken, 2015. URL: https://www.astm.org/Standards/ISOASTM52900.htm.

[14] 3D Hubs. *What is 3D Printing?- The definitive guide to additive manufacturing*. 2018. URL: https://www.3dhubs.com/what-is-3d-printing{\#}technologies (visited on 02/26/2018).

[15] Martin Baumers, Phill Dickens, Chris Tuck, and Richard Hague. "The cost of additive manufacturing: Machine productivity, economies of scale and technology-push". In: *Technological Forecasting and Social Change* 102 (2016), pp. 193–201. ISSN: 00401625. DOI: 10.1016/j.techfore.2015.02.015. URL: http://dx.doi.org/10.1016/j.techfore.2015.02.015.

[16] Brett P. Conner, Guha P. Manogharan, Ashley N. Martof, Lauren M. Rodomsky, Caitlyn M. Rodomsky, Dakesha C. Jordan, and James W. Limperos. "Making sense of 3-D printing: Creating a map of additive manufacturing products and services". In: *Additive Manufacturing* 1 (2014), pp. 64–76. ISSN: 22148604. DOI: 10.1016/j.addma.2014.08.005. URL: http://dx.doi.org/10.1016/j.addma.2014.08.005.

[17] Barry Berman. "3-D printing: The new industrial revolution". In: *Business Horizons* 55.2 (2012), pp. 155–162. ISSN: 00076813. DOI: 10.1016/j.bushor.2011.11.003. URL: http://dx.doi.org/10.1016/j.bushor.2011.11.003.

[18] GE Additive. *GE Additive Manufacturing in Alabama: The Future Is Now.* 2016. URL: https://www.ge.com/additive/press-releases/ge-additive-manufacturing-alabama-future-now (visited on 03/01/2018).

[19] New Balance. *The Future of Running is Here.* 2016. URL: https://www.newbalance.com/article?id=4041 (visited on 03/07/2018).

[20] Michelle Matisons. *Futurecraft 3D: Adidas Says It Will Turn to 3D Printed Shoes in Near Future.* 2015. URL: https://3dprint.com/99620/futurecraft-3d-adidas-shoes/ (visited on 03/07/2018).

[21] Sarah Saunders. *adidas and Carbon Announce Partially 3D Printed AlphaEDGE 4D LTD Shoe.* 2018. URL: https://www.3dprint.com/203543/adidas-carbon-alphaedge-4d-ltd/ (visited on 03/07/2018).

[22] Sung Hoon Ahn, Michael Montero, Dan Odell, Shad Roundy, and Paul K. Wright. "Anisotropic material properties of fused deposition modeling ABS". In: *Rapid Prototyping Journal* 8.4 (2002), pp. 248–257. ISSN: 1355-2546. DOI: 10.1108/13552540210441166. URL: http://www.emeraldinsight.com/doi/10.1108/13552540210441166.

[23] C. S. Lee, S. G. Kim, H. J. Kim, and S. H. Ahn. "Measurement of anisotropic compressive strength of rapid prototyping parts". In: *Journal of Materials Processing Technology* 187-188 (2007), pp. 627–630. ISSN: 09240136. DOI: 10.1016/j.jmatprotec.2006.11.095.

[24] Paul Osswald. "Comparison of Failure Criteria of Fiber Reinforced Polymer Composites". Term Thesis. Technische Universität München, 2015.

[25] C.T. Sun, B.J. Quinn, and J. Tao. "Comparative Evaluation of Failure Analysis Methods for Composite Laminates." In: *U.S. Department of Transportation* - .May (1996), p. 133. URL: http://trid.trb.org/view.aspx?id=523207.

[26] I.I Gol'denblat and V.A. Kopnov. "Strength of Glass-Reinforced Plastics in the Complex Stress State". In: *Mekhanika Polimerov* 1.2 (1965), pp. 70–78.

[27] P. Obst, M. Launhardt, D. Drummer, P. V. Osswald, and T. A. Osswald. "FAILURE CRITERION FOR SLS ADDITIVE MANUFACTURED PARTS". In: *SPE ANTEC® Anaheim 2017.* Anaheim, 2017, pp. 49–54.